Ozone-Induced Programmed Cell Death in the Arabidopsis *radical-induced cell death1* Mutant[1]

Kirk Overmyer[2], Mikael Brosché, Riikka Pellinen[3], Tero Kuittinen, Hannele Tuominen[4], Reetta Ahlfors, Markku Keinänen[5], Mart Saarma, Dierk Scheel, and Jaakko Kangasjärvi*

Department of Biological and Environmental Sciences (K.O., M.B., R.P., H.T., R.A., M.K., J.K.) and Institute of Biotechnology (K.O., R.P., T.K., H.T., M.K., M.S., J.K.), University of Helsinki, FIN–00014 Helsinki, Finland; and Department of Stress and Developmental Biology, Leibniz Institute of Plant Biochemistry, D–06120 Halle/Saale, Germany (D.S.)

Short, high-concentration peaks of the atmospheric pollutant ozone (O_3) cause the formation of cell death lesions on the leaves of sensitive plants. Numerous similarities between the plant responses to O_3 and pathogens suggest that O_3 triggers hypersensitive response-like programmed cell death (PCD). We examined O_3 and superoxide-induced cell death in the O_3-sensitive *radical-induced cell death1* (*rcd1*) mutant. Dying cells in O_3-exposed *rcd1* exhibited several of the typical morphological characteristics of the hypersensitive response and PCD. Double-mutant analyses indicated a requirement for salicylic acid and the function of the cyclic nucleotide-gated ion channel AtCNGC2 in cell death. Furthermore, a requirement for ATPases, kinases, transcription, Ca^{2+} flux, caspase-like proteolytic activity, and also one or more phenylmethylsulfonyl fluoride-sensitive protease activities was shown for the development of cell death lesions in *rcd1*. Furthermore, mitogen-activated protein kinases showed differential activation patterns in *rcd1* and Columbia. Taken together, these results directly demonstrate the induction of PCD by O_3.

Ozone (O_3) is an atmospheric pollutant that is phytotoxic via its breakdown in the apoplast to form reactive oxygen species (ROS). Short, high-concentration peaks, so-called acute O_3, cause visible damage in sensitive plants (Wohlgemuth et al., 2002). Although accumulating evidence has deepened our understanding of oxidative stress and antioxidant defenses in O_3 responses (Kangasjärvi et al., 1994; Sandermann et al., 1998; Overmyer et al., 2003), the mechanisms involved in O_3-induced cell death are still relatively unknown. Due to the strong chemical reactivity of O_3, its toxicity has previously been attributed to an ability to form toxic ROS that directly damage membranes (for review, see Heath and Taylor, 1997). However, the view of O_3 has recently shifted, where it is now regarded in many cases not as a toxin but rather as an elicitor of cell death (Sandermann et al., 1998).

O_3-induced plant responses resemble on several levels the hypersensitive response (HR), normally seen as the result of challenge by an avirulent pathogen (for review, see Rao and Davis, 2001; Langebartels and Kangasjärvi, 2004). Common to these two processes are the induction of a biphasic oxidative burst, salicylic acid (SA) accumulation, ion fluxes, the deposition of cell wall-strengthening phenolic compounds, induction of defense genes such as *Phe ammonia lyase*, *pathogenesis-related protein-1* (*PR-1*), and *glutathione S-transferase* (*GST*), as well as induction of local and systemic pathogen resistance. This has led to the view that O_3 misfires HR-like cell death and defense programs via mimicry of the oxidative burst induced by avirulent pathogens.

The HR is genetically regulated, and a form of programmed cell death (PCD; Dangl et al., 1996), where ROS have a well-established role in the induction and propagation of cell death signals, both generally and in spontaneous lesion mimic mutants (Vranová et al., 2002). As has often been stated (Kangasjärvi et al., 1994; Pell et al., 1997; Sandermann et al., 1998; Rao et al., 2000a), the similarities between the plant responses during the HR and under O_3 suggest that O_3-induced cell death is executed by the same mechanisms as the HR. This makes O_3 a convenient probe for the study of ROS-induced PCD and implies that radical hypersensitive mutants, such as *radical-induced cell death1* (*rcd1*; Overmyer et al., 2000;

[1] This work was supported by the Academy of Finland (grant nos. 43671 and 37995), by the Finnish Centre of Excellence Programme (2000–2005), and by an Academy of Finland/German Academic Exchange Service grant (SA10256/313–SF–PPP–pz). R.P. was supported by the Finnish Graduate program in Environmental Physiology, Molecular Biology, and Ecotechnology, the University of Kuopio, and The Finnish Graduate School in Environmental Science and Technology, Åbo Akademi.

[2] Present address: Biology Department, CB No. 3280, University of North Carolina, Chapel Hill, NC 27599–3280.

[3] Present address: A.I. Virtanen Institute, University of Kuopio, FIN–70211 Kuopio, Finland.

[4] Present address: Umeå Plant Science Centre, Department of Plant Physiology, Umeå University, SE–90187 Umeå, Sweden.

[5] Present address: Department of Biology, University of Joensuu, PO Box 111, FIN–80101 Joensuu, Finland.

* Corresponding author; e-mail jaakko.kangasjarvi@helsinki.fi; fax 358–9–191–59552.

Article, publication date, and citation information can be found at www.plantphysiol.org/cgi/doi/10.1104/pp.104.055681.

Ahlfors et al., 2004a), represent a new class of lesion mimic mutants.

Although it is generally stated that O_3 can induce PCD (Rao et al., 2000a), the morphological and biochemical hallmarks of PCD in O_3-exposed plants have only been described in tobacco (*Nicotiana tabacum*; Pasqualini et al., 2003). In this article, we have deepened the view with the use of various O_3-sensitive and hormonal mutants of Arabidopsis (*Arabidopsis thaliana*), such as *rcd1*, *jasmonate resistant1* (*jar1*), *nonexpresser of PR proteins1* (*npr1*), and transgenic NahG plants, to study the mechanisms of O_3-induced cell death. In addition, we have addressed in more detail the question of O_3-induced PCD by characterizing morphological similarities to the HR and PCD and showing the requirement for active metabolism in the ROS-induced cell death in *rcd1*.

RESULTS

The Morphology of O_3-Induced Cell Death

Two alleles of *rcd1* have been found in ROS-related mutant screens and have been introduced previously (Overmyer et al., 2000; Ahlfors et al., 2004a; Fujibe et al., 2004). *rcd1* is sensitive to O_3, which already can be measured as increased ion leakage at 2 h and maximum at 12 to 24 h after the beginning of an O_3 exposure (Overmyer et al., 2000). The morphology of O_3-induced cell death was further studied in *rcd1* and parental wild-type Columbia (Col-0) 24 h after the beginning of an O_3 exposure (250 nL L^{-1}, 8 h), when the difference in cell death between these two genotypes is maximal. In Col-0 plants, no visible damage was apparent (Fig. 1A) when *rcd1* formed macroscopic cell death lesions (Fig. 1E). Lesions in *rcd1* take the form of either defined HR-like foci or large confluent areas of dry, collapsed tissue that resemble disease symptoms.

Although free of macroscopic lesions, O_3-exposed Col-0 exhibited a small number (10–30/leaf) of microscopic lesions. These individual or small groups of cells accumulated autofluorescent phenolics (Fig. 1B, arrow) and were frequently in the vicinity of the vascular bundles. In contrast, O_3-induced lesions in *rcd1* exhibited a strong accumulation of autofluorescent phenolic compounds (Fig. 1F, asterisk). Lesion induction and autofluorescent phenolic accumulation were specific, O_3-triggered events in these experiments, as all clean-air control samples did not display these symptoms.

One of the biochemical characteristics of PCD is the controlled degradation of nuclear DNA into internucleosomal fragments (Dangl et al., 1996), which can be detected with the terminal-transferase dUTP nuclear end label (TUNEL) assay via labeling of the free 3′ ends liberated in nuclei undergoing DNA degradation. The vast majority of O_3-exposed Col-0 leaf sections examined were free of TUNEL staining (Fig. 1C).

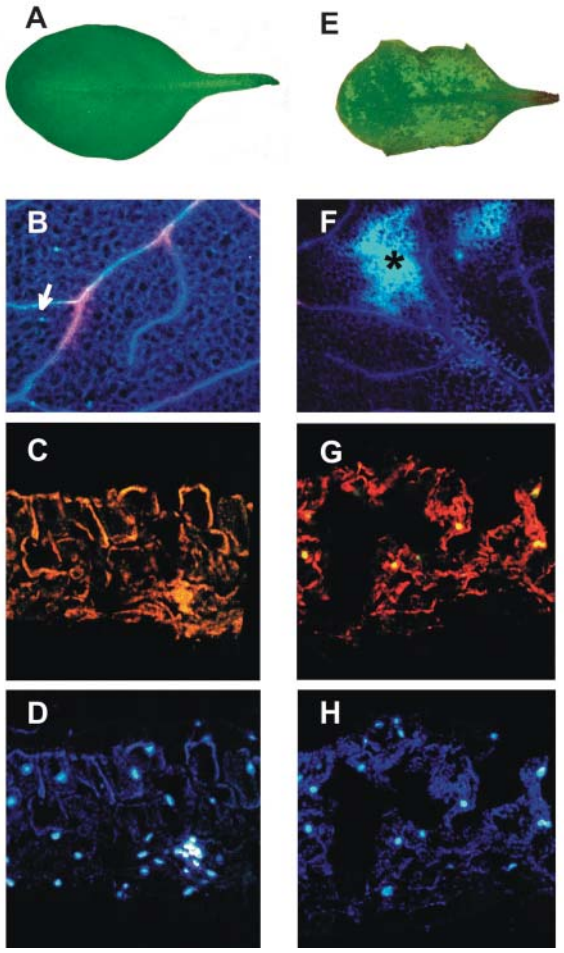

Figure 1. O_3-induced HR-like lesions exhibit PCD hallmarks. O_3-exposed Col-0 (A–D) and *rcd1* (E–H) leaves at 24 h (A, B, E, and F) and 8 h (C, D, G, and H) after the beginning of the exposure (250 nL L^{-1}, 8 h). Leaves show the absence in Col-0 (A) and the presence in *rcd1* (E) of O_3-induced lesions. Autofluorescence micrographs visualize the deposition of phenolic compounds indicating the activation of HR-like cell death and defenses seen in a few individual cells (arrow) exhibiting microscopic HR-like cell death in Col-0 (B) and in large tissues of *rcd1* (F, asterisk). DAPI stain (D and H) depicts all nuclei for comparison to TUNEL-stained sections (C and G), illustrating the absence in Col-0 (C) and the presence in *rcd1* (yellow-green stain, G) of nuclei undergoing DNA fragmentation.

However, consistent with the low level of microscopic cell death observed by fluorescence microscopy in O_3-exposed Col-0 leaves, a few TUNEL-positive nuclei were found especially in or around the vascular bundles in Col-0 (data not shown) when O_3-exposed *rcd1* had a high proportion of TUNEL-positive nuclei (Fig. 1G). All parallel clean-air control sections of both genotypes and controls lacking the terminal transferase were free of TUNEL-positive nuclei, indicating the specificity of the assay. At higher magnification (data not shown), the TUNEL-negative nuclei in *rcd1* appeared larger and the 4′6-diamino-phenylindole (DAPI) stain more even and diffuse. In contrast,

TUNEL-positive nuclei were smaller and contained brightly stained foci, indicative of nuclear shrinkage and chromatin condensation, two additional characteristics of PCD.

The ultrastructure of *rcd1* nuclei undergoing cell death was examined by transmission electron microscopy. Figure 2 shows typical Col-0 (A) and *rcd1* (C) nuclei from healthy clean-air control sections and from leaves sampled at 10 h after the beginning of a 6-h O_3 exposure (250 nL L^{-1}; B and D). A nucleus from a dying cell within an O_3-induced lesion of *rcd1* was shrunken and generally more electron dense (Fig. 2D) and contained dark patches of condensed chromatin (arrows). Nuclei from O_3-exposed Col-0 leaves had a normal morphology (Fig. 2B), indicating that the changes observed in *rcd1* were specific to cell death lesions and not a general effect of O_3 exposure. Healthy nuclei (A–C) were typically suspended in the cytoplasm, while nuclei from dying cells in O_3-exposed *rcd1* were frequently found adjacent to the plasma membrane, as shown in Figure 2D. Cells within the O_3-induced lesions also frequently displayed vesiculation of the cytosol. In Figure 2D, a fully formed vesicle and a small vesicle in the vicinity of the plasma membrane can be seen.

Based on these results, it can be concluded that the cell death in O_3-exposed *rcd1* exhibits nuclear DNA fragmentation, nuclear shrinkage, chromatin condensation, and cytosol vesiculation, all of which are characteristic of PCD (Dangl et al., 1996; Mittler et al., 1997). None of these features were seen in the O_3-tolerant Col-0.

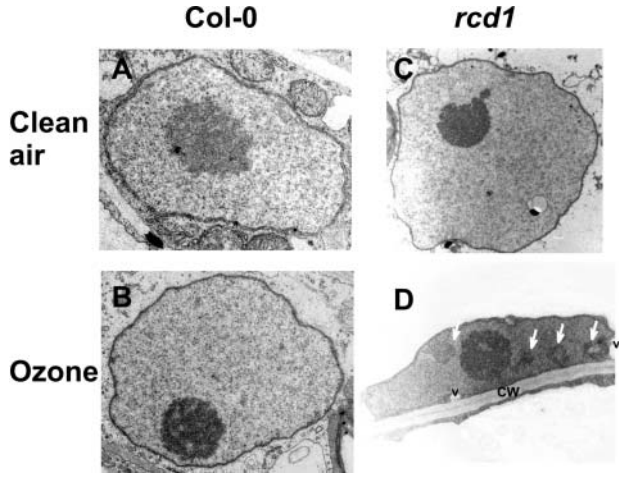

Figure 2. *rcd1* nuclear morphology. Transmission electron micrographs of Col-0 (A and B) and *rcd1* (C and D) nuclei. A and C, Nuclei from healthy leaves in the clean-air controls. B, Typical nucleus from O_3-exposed Col-0. D, Nucleus in a *rcd1* cell undergoing PCD from section through an O_3-induced lesion. B and D, Taken from leaves sampled at 10 h after the beginning of a 6-h, 250 nL L^{-1} O_3 exposure. Arrow in D indicates aggregates of condensed chromatin. v, Vesicles; cw, cell wall.

Mutant Analysis of the Role of SA, Jasmonic Acid, and HR

SA and jasmonic acid (JA) have been proposed to regulate plant PCD (Overmyer et al., 2003; Lam, 2004). To address the relationship between cell death and SA accumulation in *rcd1*, it was crossed with both SA-deficient transgenic NahG plants and the SA-insensitive *npr1*, and O_3 sensitivity of the double mutants was evaluated 7 h after the beginning of an O_3 exposure (250 nL L^{-1}, 6 h). As shown in Figure 3A, both NahG and *npr1* reduced, but did not abolish, O_3 sensitivity of *rcd1*; the double mutants *rcd1* NahG and *rcd1 npr1* were significantly less O_3 sensitive than *rcd1*, but significantly more sensitive than Col-0, *npr1*, or NahG. The JA-insensitive mutants *jar1* and *coronative insensitive 1* (*coi1*) have previously been shown to be O_3 sensitive due to defective lesion containment (Overmyer et al., 2000; Rao et al., 2000b; Tuominen et al., 2004). To gain further insight into the role of JA, *rcd1* was crossed with *jar1* and the O_3 sensitivity of the double mutant was evaluated 7 h after the beginning of an O_3 exposure (300 nL L^{-1}, 6 h; Fig. 3B). The *rcd1 jar1* double mutant displayed substantially increased O_3 damage when compared to the corresponding single mutants, further supporting the importance of JA in lesion containment. The absolute values of ion leakage differ to some extent in *rcd1* between the experiments presented in Figure 3, A to C. This is a result of normal variation in O_3 delivery kinetics in the growth chambers between different experiments.

If the cell death in *rcd1* is a result of PCD similar to the HR seen after infection with avirulent pathogens, it would be expected that a double mutant of *rcd1* with a mutant blocked in the development of HR has a reduced number of lesions following O_3 exposure. Thus, a mutant impaired in developing HR, *defense, no death* (*dnd1*), was analyzed. The *dnd1* mutant fails to develop HR as a response to avirulent Pseudomonas infection (Clough et al., 2000). *rcd1* was crossed with *dnd1* and the double mutant was exposed to O_3. In clean-air controls, *dnd1* and *rcd1 dnd1* sometimes displayed a slightly higher degree of cell death than Col-0 due to the spontaneous lesions (Clough et al., 2000) caused by the *dnd1* mutation (data not shown). However, 7 h after the beginning of an O_3 exposure (300 nL L^{-1}, 6 h), the *rcd1 dnd1* double mutant had the same level of damage as the clean-air controls, indicating that the *dnd1* mutation blocks cell death in O_3-exposed *rcd1* (Fig. 3C).

O_3-Induced Accumulation of SA, JA, and Changes in Gene Expression

Many lesion mimic mutants contain high amounts of SA under control growth conditions (Lorrain et al., 2003). To check the possibility that altered SA or JA biosynthesis was involved in the increased cell death of *rcd1*, the levels of SA (free and conjugated) and JA were analyzed in Col-0 and *rcd1* in clean-air and

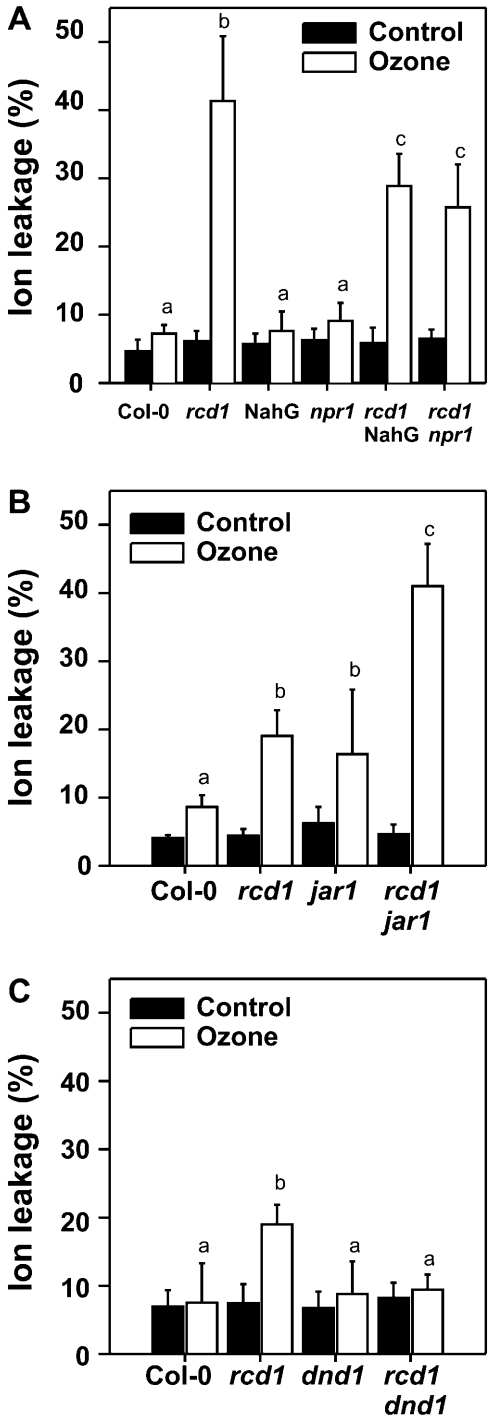

Figure 3. O_3 sensitivity of double mutants. Plants of the indicated genotypes were exposed to a single 6-h pulse of 250 nL L^{-1} of O_3 (A) or 300 nL L^{-1} (B and C), and cell death was monitored as ion leakage at 7 h after the beginning of the exposure. NahG plants express a bacterial salicylate hydroxylase gene and thus are unable to accumulate SA. Mutant *npr1* is SA insensitive and *jar1-1* is JA insensitive. The *dnd1* mutant does not develop HR as a response to avirulent Pseudomonas infection. Experiments have been replicated at least twice with similar results; one representative experiment is shown. All data points are mean ± SD (n = 5–10). Bars labeled with a different letter differ significantly ($P < 0.01$) by Tukey's honestly significant difference post-hoc test.

O_3-exposed samples. As previously reported (Rao et al., 2000b), O_3 exposure increased the levels of SA and JA in wild-type Col-0 (the latter is masked by the huge increase of JA in *rcd1*). In contrast to several other lesion mimic mutants, *rcd1* had normal levels of SA and JA under control conditions (Fig. 4). However, in the O_3-exposed *rcd1* plants, the levels of both free and conjugated SA and JA were higher than in Col-0 (Fig. 4).

SA and JA are known regulators of defense gene expression. Thus, defense gene expression was investigated in Col-0 and *rcd1* 8 h after the beginning of an

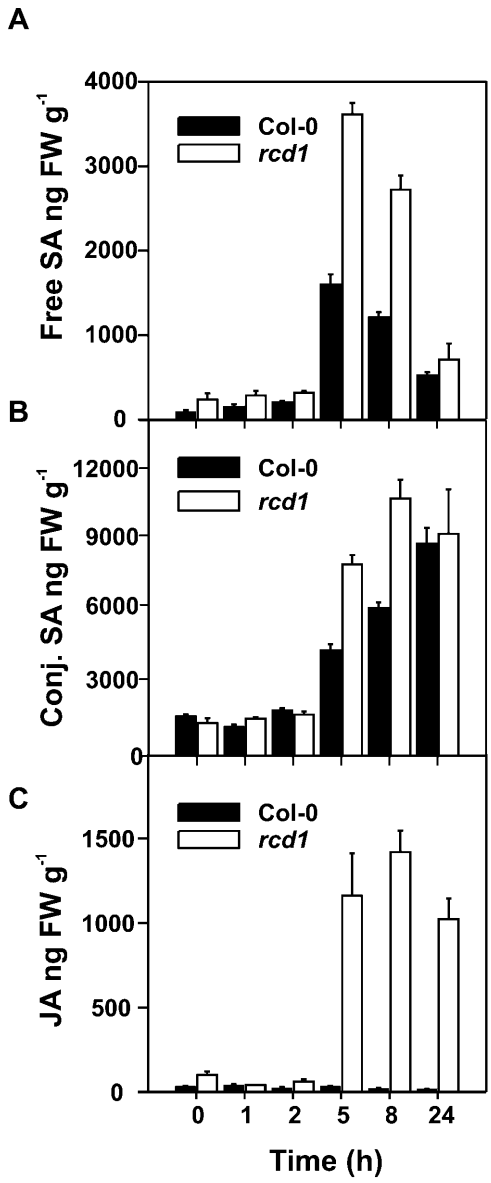

Figure 4. SA and JA levels in O_3-exposed *rcd1* and Col-0. O_3 induced accumulation of SA and JA. Free SA (A), conjugated SA (B), and JA (C) were measured in whole rosettes of Col-0 and *rcd1* in response to a single 6-h pulse O_3 exposure of 300 nL L^{-1}. The results represent means ± SE (n = 5). The analysis was repeated twice with similar results for the different genotypes.

O_3 exposure (250 nL L^{-1}, 6 h) using a customized macroarray (Table I). In accordance with the increased levels of SA (Fig. 4A) and ethylene (Overmyer et al., 2000; Tuominen et al., 2004) during O_3 exposure, ethylene and SA-regulated genes, such as *wall-associated kinase1* (*WAK1*), *PR-1*, and *GST* (SA markers) and 1-aminocyclopropane-1 carboxylic acid (ACC) oxidase, hevein-like protein, and basic chitinase (ethylene markers), had substantially higher mRNA levels in the O_3-exposed plants. Transcript levels for *PDF1.2a*, a combined ethylene/JA marker, also increased. For most genes, the differences in expression between *rcd1* and Col-0 were rather limited, with a few exceptions. ACC oxidase, hevein-like protein, and basic chitinase gene expression were increased 2 to 3 times in *rcd1* compared to Col-0. This likely reflected the higher ethylene emission (Overmyer et al., 2000) from *rcd1* during O_3 exposure.

The Role of Proteases in ROS-Induced Cell Death of *rcd1*

Proteases have both degenerative and signaling roles during PCD. In mammals, caspases (Cys aspartic proteases) are central to the regulation of PCD. Plants do not possess classic mammalian caspases; instead, they use vacuolar processing enzymes (VPEs), proteases with caspase activity, as regulators of PCD (Hatsugai et al., 2004; Rojo et al., 2004). To study the role of various types of proteases, in vitro experiments were performed. Col-0 and *rcd1* leaves were incubated with known protease inhibitors, summarized in Table II, with and without the exogenous superoxide generating system, xanthine and xanthine oxidase (XXO; Jabs et al., 1996), which has previously been shown to have a similar effect on *rcd1* as O_3 (Overmyer et al., 2000). As seen in Figure 5, both z-VAD-fmk (general caspase inhibitor 1; Garcia-Calvo et al., 1998) and phenylmethylsulfonyl fluoride (Ser-protease inhibitor) reduced the level of XXO-induced ion leakage in *rcd1* to approximately the levels of the Col-0 plants. In contrast, pepstatin, an aspartic protease inhibitor, and E-64, a Cys-protease inhibitor, had no effect. In control experiments with XXO-treated Col-0, the same inhibitors had no effect (data not shown). Therefore, it can be concluded that Ser- and caspase-like protease activities were required for execution of the superoxide-induced cell death in *rcd1*.

Cell Death Induced by O_3 and ROS Requires Active Metabolism

Inhibitors of active metabolism (Table II) were applied in planta by spraying intact *rcd1* and Col-0 prior to a 250-nL L^{-1} O_3 exposure. Cell death was monitored as ion leakage over a short time course at 0, 3, and 6 h. At these time points, ion leakage in plants that received the inhibitor treatments alone (in clean air) did not deviate from control values in Col-0 or *rcd1* (data not shown), indicating that the inhibitors were nontoxic. As shown in Figure 6A, after 3 h of O_3, the calcium channel blocker lanthanum, the transcriptional inhibitor α-amanitin, the Tyr kinase inhibitor herbimycin A, and the Ser/Thr kinase inhibitor K252a caused a statistically significant reduction ($P < 0.05$) in ion leakage in *rcd1* as compared to O_3 alone. Furthermore, at 6 h, herbimycin A, K252a, lanthanum, and α-amanitin pretreatments significantly diminished O_3-induced ion leakage in *rcd1*. In Col-0, pretreatment with herbimycin

Table I. *Expression of selected stress- and defense-related genes in wild-type Col-0 and rcd1*

The samples were harvested 8 h after beginning of a 6-h O_3 exposure of 250 nL L^{-1} O_3. The values depict the average ratios of mRNA abundance between O_3-treated and clean-air-grown material from two biological repeats. The data from the macroarray were first normalized to the mean of mRNA abundance of actin genes *ACT2* (At3g18780) and *ACT8* (At1g49240), which were shown to be constitutively expressed by RNA gel blots. A complete list of the genes used can be seen at http://www.helsinki.fi/biosci/plantstress/contents/publications/macroarray.html.

AGI Code	Annotation	Col-0	*rcd1*
At3g12500	Basic chitinase	7.8	20.3
At1g62380	ACC oxidase 2	2.2	5.4
At1g32210	Defender against death1 (*dnd1*)	4.3	3.4
At2g47730	glutathione *S*-transferase 6 (*GST6*)	2.0	3.9
At5g44420	Plant defensin (PDF1.2a)	7.8	3.1
At4g02520	Glutathione *S*-transferase, putative	26.8	63.9
At2g14610	Pathogenesis-related protein-1 (*PR-1*)	65.0	69.1
At3g04720	Hevein-like protein	10.3	30.8
At1g02930	Glutathione *S*-transferase, putative	18.1	24.8
At3g49120	Peroxidase, putative	7.2	5.6
At5g20230	Plastocyanin-like domain-containing protein	63.1	47.2
At5g39580	Peroxidase	5.1	4.4
At1g21250	Wall-associated kinase1 (*WAK1*)	2.9	7.7
At3g15350	Legume lectin family protein	10.2	15.3
At5g54810	Trp synthase β-subunit	3.7	5.1

Table II. *Inhibitors used in this study*[a]

Symbol[b]	Inhibitor/Reagent[c]	Target/Effect[d]	Infiltrate XXO	Spray O_3
			μM[e]	μM[f]
Van	Metavanadate	ATPases	50,000	100,000
Lan	$LaCl_3$	Ca^{2+} channels	1,000	2,000
Ama	α-Amanitin	Transcription	2.2	4.4
Hba	Herbimycin A	Tyr kinases	1,000	2,000
K25	K252a	Ser/Thr kinases	2.2	4.4
Pep	Pepstatin	Asp proteases	1.0	
E-64	E-64	Cys proteases	1.0	
VAD	z-VAD-fmk	Caspases	50	
PMSF	PMSF	Ser proteases	500	
Ion	A23187	Ca^{2+} ionophore	10	
Ca	$CaCl_2$	Increased Ca^{2+}	2,000	
Mg	$MgCl_2$	Control	2,000	
EGTA	EGTA	Decreased Ca^{2+}	1,000	
Gd	$Gd(III)Cl_3$	Ca^{2+} channels	1,000	

[a]Inhibitors used in this study with their respective abbreviations, concentrations used, and proposed targets. [b]Abbreviations used in the figures for each inhibitor. [c]Full name of all inhibitors and reagents used. [d]Proposed inhibitor target or the expected effect of the treatments. [e]Concentrations used for in vitro coinfiltration experiments with XXO as the radical source. [f]Concentrations used for pretreating plants by spraying intact plants with the inhibitor 1 h prior to O_3 exposure.

A, K252a, lanthanum, α-amanitin, or metavanadate did not result in significant deviation from fumigation with O_3 alone (Fig. 6B). In similar in vitro experiments using XXO instead of O_3 as the death-inducing stimulus, comparable results were obtained with both Col-0 and *rcd1* (data not shown).

The fact that inhibition of protein kinases with K252a and herbimycin A reduced cell death in *rcd1* prompted us to assess the effect of the protein phosphatase inhibitor calyculin A. Table III shows that treatment with calyculin A triggered a 5-fold increase in cell death in *rcd1*. In Col-0, calyculin A caused a slight, but statistically nonsignificant, increase in ion leakage.

Calcium- and ROS-Induced Cell Death

We have shown above that O_3- and superoxide-induced cell death was attenuated by the calcium channel blocker lanthanum (Fig. 6A). To further elucidate the role of calcium, the effect of increased calcium flux was tested in XXO-challenged leaves with calcium ionophore A23187 and increased extracellular calcium levels (2 mM $CaCl_2$). These treatments, or the control treatment with Mg^{2+}, did not cause statistically significant changes in XXO-induced ion leakage in *rcd1* (Fig. 7A) or Col-0 (Fig. 7B) leaves. A reduction in calcium fluxes either by the chelation of extracellular calcium with EGTA or the use of calcium channel blockers lanthanum and gadolinium, however, caused a significant reduction in the XXO-induced ion leakage in *rcd1* (Fig. 7A), suggesting that calcium influx from the apoplast is involved in the regulation of cell death in *rcd1*. In the ROS-tolerant Col-0, differences in cell death after the restriction of calcium flux were not statistically significant (Fig. 7B).

O_3 Induces Rapid Activation of Mitogen-Activated Protein Kinases

Application of the Ser/Thr kinase inhibitor K252a decreased O_3-induced cell death in *rcd1* (Fig. 6). Since K252a acts as a competitive inhibitor of ATP for various kinases, including mitogen-activated protein (MAP) kinases, we assessed MAP kinase activation in *rcd1* and Col-0 during O_3 exposure. Protein extracts from O_3-exposed *rcd1* and Col-0 were analyzed with an antibody (anti-phospho-TEY) that detects the activated forms of both mammalian and plant MAP kinases where the Thr and Tyr residues in the activation loop are phosphorylated (Chang and Karin, 2001; Asai et al., 2002). Two putative MAP kinases of approximately 43 and 45 kD were activated in O_3-treated tissue when compared to clean-air-grown plants (Fig. 8A). These two kinases, which have been identified with specific antibodies as AtMPK3 and AtMPK6 (Ahlfors et al., 2004b), were activated transiently during O_3 exposure with slight differences between Col-0 and *rcd1*; in Col-0, 45-kD kinase showed the highest phosphorylation level 1 h after the start of the exposure, whereas in *rcd1*, stronger phosphorylation of 45-kD kinase was already evident 0.5 h after the start of the exposure. Immunoprecipitation kinase assays with the specific antibodies against AtMPK3 and AtMPK6 revealed that, indeed, *rcd1* had an earlier peak activity of AtMPK6 (at 0.5 h) and a slightly lower peak activity of AtMPK3 (at 1–2 h) when compared to Col-0. When the AtMPK3 and AtMPK6 protein

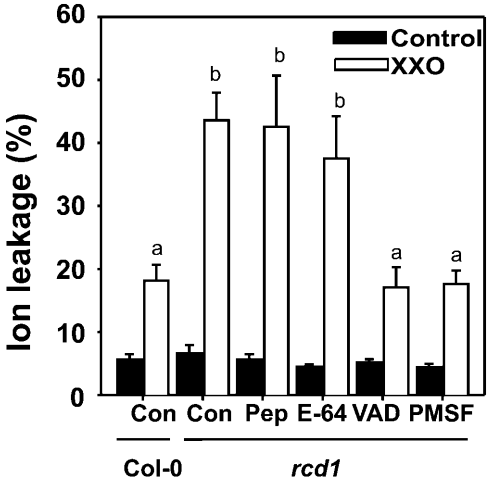

Figure 5. Effect of protease inhibitors on superoxide-induced cell death. Col-0 and *rcd1* plants were treated in vitro with a panel of protease inhibitors in the presence and absence of a XXO superoxide-generating system. Cell death was monitored as ion leakage. Inhibitors used, their abbreviations, and targets were as follows: Pep, pepstatin, aspartic proteases; E-64, Cys proteases; VAD, z-VAD-fmk (caspase inhibitor 1), caspases; PMSF, phenylmethylsulfonyl fluoride, Ser proteases. Inhibitor information with concentrations used is summarized in Table II. Inhibitor treatment of Col-0 plants resulted in no deviation from control and XXO-treated values (data not shown). Experiments have been replicated twice with similar results; one representative experiment is shown. All data points are mean ± SD ($n = 5$). Bars labeled with a different letter differ significantly ($P < 0.01$), according to Tukey's honestly significant difference post-hoc test.

accumulation was analyzed, no differences between *rcd1* and Col-0 were found (data not shown).

DISCUSSION

Morphological Markers of PCD Are Induced by O_3

The atmospheric pollutant O_3 induces cell death in sensitive individuals of several species (Koch et al., 2000; Wohlgemuth et al., 2002; Pasqualini et al., 2003). Typically, Arabidopsis mutants, in which a component required for either antioxidative capacity or a process that controls cell death is deficient, are sensitive to O_3 (Rao et al., 2000a; Overmyer et al., 2003; Langebartels and Kangasjärvi, 2004). One such Arabidopsis mutant, *rcd1*, was isolated based on the extensive cell death seen in middle-aged rosette leaves as a result of O_3 exposure (Overmyer et al., 2000). *RCD1* encodes a protein that most likely is involved in interactions between hormonal signaling cascades in abiotic stress (Ahlfors et al., 2004a). In this study, we used different experimental approaches to dissect processes involved in O_3-induced PCD using the *rcd1* mutant. O_3-induced lesions in *rcd1* were large, whereas the wild-type Col-0 had microscopic cell death. In both accessions, O_3 caused an accumulation of autofluorescent phenolic compounds in and around the dying cells (Fig. 1). This response is also triggered by wounding or a resistance gene (*R*-gene) product upon recognition of an avirulent pathogen (Dietrich et al., 1994). In addition, the cell death in O_3-exposed *rcd1* exhibits nuclear DNA fragmentation, nuclear shrinkage, chromatin condensation, and cytosol vesiculation (Figs. 1 and 2), all of which are morphological and functional characteristics of PCD.

PCD is an orderly and highly regulated disassembly of cellular functions. It requires active cellular processes, such as energy production, signal transduction, ion fluxes, transcription, and translation. Active cell death has been demonstrated with the use of pharmacological inhibitors in response to pathogens (He et al.,

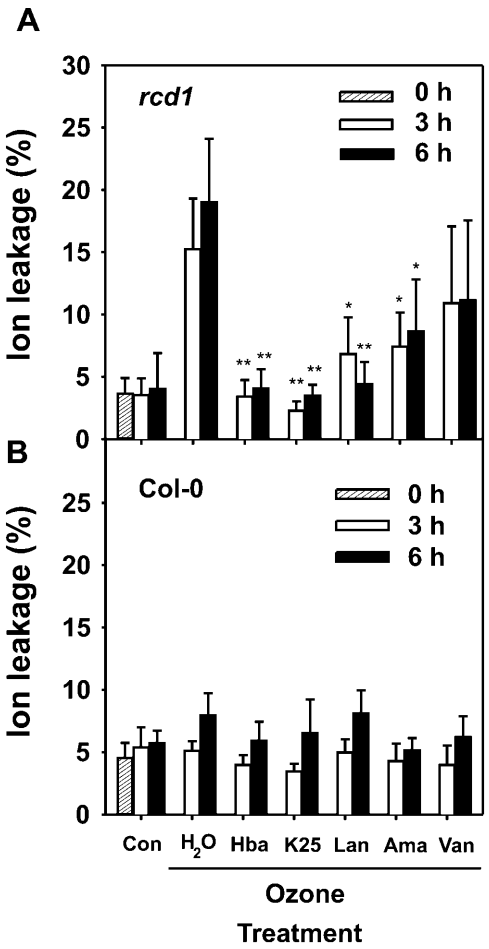

Figure 6. Effect of pharmacological inhibitors on O_3-induced cell death. A, *rcd1* and B, Col-0 plants were pretreated 1 h prior to exposure by spraying intact plants with inhibitor solutions followed by an exposure to 250 nL L^{-1} O_3, and cell death was monitored as ion leakage from leaves collected at 3 and 6 h after the beginning of the 6-h exposure. Inhibitors used, their abbreviations, and targets were as follows: Hba, herbimycin A, Tyr-kinases; K25, K252a, Ser/Thr-kinases; Lan, lanthanum chloride, calcium channels; Ama, α-amanitin, transcription; Van, sodium metavanadate, ATPases. Inhibitor information with concentrations used is summarized in Table II. Experiments have been replicated twice with similar results; one representative experiment is shown. All data points are mean ± SD ($n = 5$). Bars marked with an asterisk (*) or double asterisks (**) were significantly different from the control at the $P < 0.05$ or $P < 0.01$ level, respectively, according to Tukey's honestly significant difference post-hoc test.

Table III. *Induction of cell death by calyculin A*

	Control[a]	Calyculin A[a]
Col-0	7.95 ± 1.46[b]	14.19 ± 3.80[b]
rcd1	5.90 ± 1.13[b]	30.74 ± 10.49[c]

[a]Values given are percent ion leakage ± SD ($n = 5$) induced by 100 μM calyculin A measured at 18 h posttreatment. [b,c]Values followed by the same letter do not differ significantly for each other ($P < 0.05$), according to Tukey's honestly significant post-hoc test.

1993), H_2O_2 (Levine et al., 1996), high light in antisense catalase tobacco (Dat et al., 2003), and O_3 (this study). The inhibitors used, however, are not generally specific for only one process and the unambiguous demonstration that a process is used (e.g. in PCD) requires additional ways of verification, such as mutant analysis.

The Role of Hormones

SA accumulation is a requirement for the execution of HR-like cell death and for the development of systemic acquired resistance (Durner et al., 1997). O_3-exposed *rcd1* had increased SA concentration when compared to Col-0 (Fig. 4A), and SA was required for O_3 lesion formation in *rcd1*, since compromised SA signaling in *rcd1 npr1* and *rcd1* NahG double mutants diminished symptom development significantly, but not completely (Fig. 3A). This suggests that O_3-induced cell death in *rcd1* comprises both SA-dependent and SA-independent components. SA-dependent cell death may be taken as further evidence of O_3-induced HR-like PCD. Cell death in several lesion mimic mutants is reduced in double mutants with compromised SA signaling, similarly suggesting a role for SA in lesion development (Lorrain et al., 2003).

JA has a proposed role in lesion containment during O_3 exposure (Overmyer et al., 2003; Tuominen et al., 2004). Treatment of O_3-sensitive accessions (Arabidopsis mutant *rcd1* and the ecotype Cape Verdi Islands (Cvi-0); tobacco Bel-W3) with methyl jasmonate reduced or abolished O_3-induced cell death, and JA-insensitive or biosynthesis mutants (*jar1*, *coi1*, and *fad3/7/8*) displayed lesions following O_3 exposure (Örvar et al., 1997; Overmyer et al., 2000; Rao et al., 2000b; Tuominen et al., 2004). JA levels increased dramatically in O_3-exposed *rcd1* (Fig. 4B). It has been proposed that the increase in JA accumulation in O_3-exposed plants is a result of the cell death process itself, which causes a release of a substrate for JA biosynthesis from the membranes of the damaged cells (Vahala et al., 2003; Tuominen et al., 2004). This would form an autocatalytic containment mechanism for the lesion propagation where the magnitude of cell death would also determine the strength of signal for lesion containment by JA. By this mechanism, decreased JA sensitivity will also increase sensitivity to O_3, which was apparent in the *rcd1 jar1* double mutant that displayed higher lesion formation than either parent. A similar result was observed when the lesion mimic mutant *hypersensitive response-like lesions1* (*hrl1*) was crossed with *coi1*; the resulting double mutant was unable to contain lesions and had exaggerated cell death (Devadas et al., 2002).

Inhibitor Studies

The inhibitor studies indicated a role for caspases and calcium in the induction of cell death by ROS in *rcd1* (Figs. 5–7). Caspases are central to the regulation of PCD in mammals. Attempts to find similar proteins

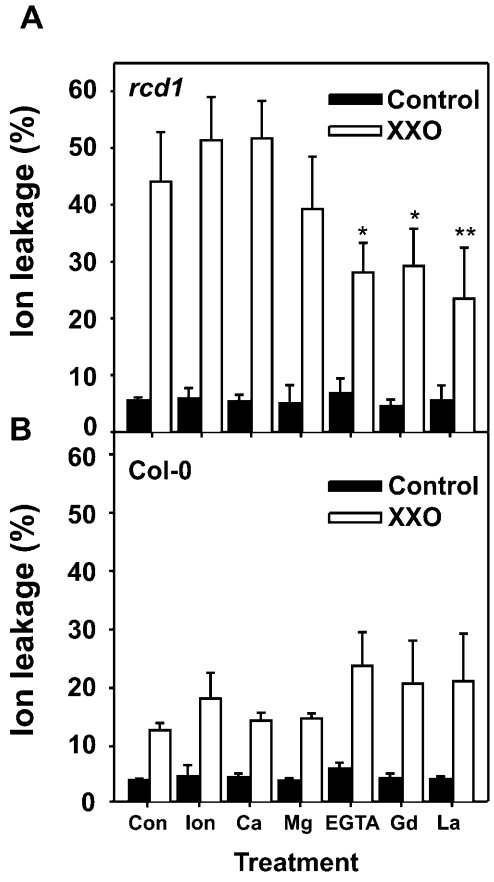

Figure 7. Effect of altered calcium flux on superoxide-induced cell death. A, *rcd1* and B, Col-0 plants were treated in vitro with reagents to alter calcium flux in the presence and absence of a XXO superoxide-generating system. Cell death was monitored as ion leakage. Reagents used, their abbreviations, and targets were as follows: Ion, A23187, calcium ionophore; Ca, calcium chloride, increased extracellular calcium; Mg, magnesium chloride, divalent cation control; EGTA, chelator of extracellular calcium; Gd, gadolinium(III) chloride, calcium channel blocker; La, lanthanum chloride, calcium channel blocker. Inhibitor and reagent information and concentrations used are summarized in Table II. Experiments have been replicated twice with similar results; one representative experiment is shown. All data points are mean ± SD ($n = 5$). Bars marked with an asterisk (*) or double asterisks (**) were significantly different from the water control at the $P < 0.05$ or $P < 0.01$ level, respectively, according to Tukey's honestly significant difference post-hoc test.

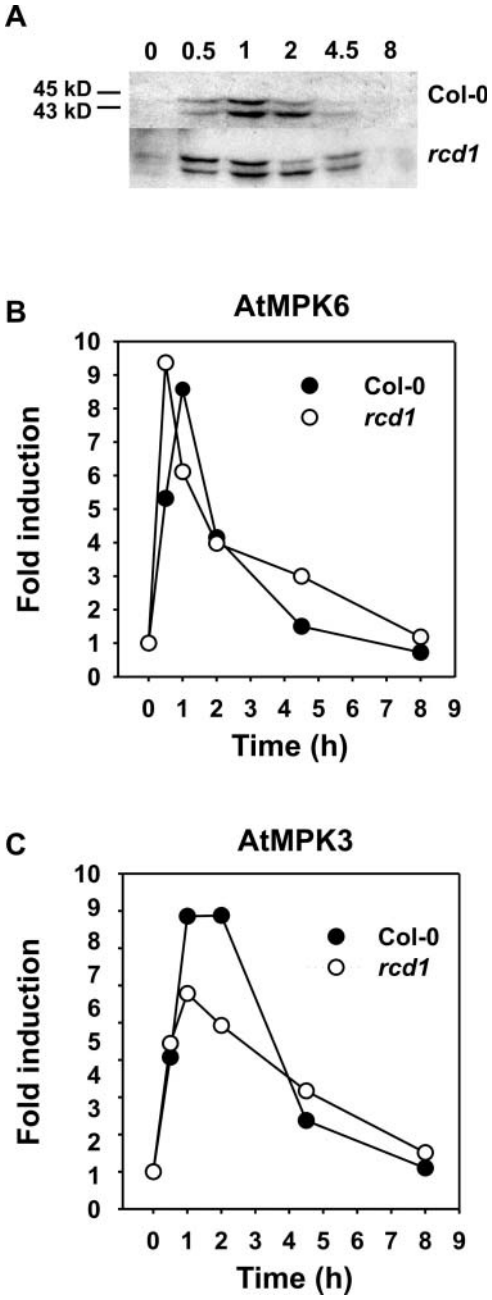

Figure 8. MAP kinase activity in *rcd1* and Col-0. A, O_3-induced MAP kinase activation in Col-0 and *rcd1*. Activated MAP kinases were detected in the wild-type Col-0 and *rcd1* mutant by western blotting using an anti-phospho-TEY motif antibody, which recognizes the phosphorylated activation loop. Col-0 and *rcd1* were exposed to 7 h of O_3 (250 nL L^{-1}) and samples collected at 0, 0.5, 1, 2, 4.5, and 8 h. B and C, Immunoprecipitation kinase assay with AtMPK6 (B) and AtMPK3 (C) antibodies. Protein samples from O_3-exposed (7 h, 250 nL L^{-1}) Col-0 and *rcd1* plants were immunoprecipitated with AtMPK3 and AtMPK6 antisera. Leaf samples were collected at 0, 0.5, 1, 2, 4.5, and 8 h after the beginning of the exposure. Results are expressed as fold induction of myelin basic protein phosphorylating activity compared to myelin basic protein phosphorylation activity in leaf extracts from clean-air-grown plants.

in plants have failed, although plants have been suggested to use the related protein family of metacaspases as regulators of cell death (Watanabe and Lam, 2004). However, measurements of metacaspase activity indicate that they are not directly responsible for earlier reported caspase-like activities in plants (Vercammen et al., 2004). Recently, Cys proteases belonging to the class of VPEs have been shown to be regulators of virus-induced PCD in tobacco (Hatsugai et al., 2004), and bacterial, fungal, and virus-induced PCD in Arabidopsis (Rojo et al., 2004). VPEs display caspase activity and are inhibited by caspase inhibitors (Hatsugai et al., 2004; Rojo et al., 2004). Superoxide-induced cell death in *rcd1* was reduced by treatment with the caspase inhibitor z-VAD-fmk (Fig. 5), suggesting that an Arabidopsis VPE might be involved in the regulation of PCD in *rcd1*.

O_3 is a demonstrated inducer of calcium ion fluxes (Castillo and Heath, 1990; Clayton et al., 1999). Calcium is also required for activation of the NADPH oxidase (Bowler and Fluhr, 2000). Cell death in *rcd1* was inhibited by diphenylene iodonium, suggesting an involvement of the NADPH oxidase in cell death activation (Overmyer et al., 2000). Thus, involvement in the activation of the NADPH oxidase presents one mechanism by which calcium influx could regulate cell death in *rcd1*. Chelation of extracellular calcium with EGTA has also been shown to release intracellular calcium in the cytosol (Cessna and Low, 2001). An alternative interpretation for the reduction of cell death in XXO + EGTA-treated *rcd1* (Fig. 7A) could be that cytosolic calcium release leads to partial inhibition of PCD. The lack of O_3-induced cell death in the *rcd1 dnd1* double mutant further supports a requirement for cations, K^+ or Ca^{2+}, in the cell death in *rcd1*. The *dnd1* mutant bears a mutation in a cyclic nucleotide-gated cation channel AtCNGC2 and fails to produce HR in response to pathogen infections (Clough et al., 2000). AtCNGC2 has previously been shown to be able to transport K^+ or Ca^{2+} (Leng et al., 1999, 2002). Since the *dnd1* mutant also has elevated SA levels and constitutively activated defenses (Clough et al., 2000), an alternative explanation for the lack of increased cell death in *rcd1 dnd1* could be that the SA-dependent constitutive defenses are sufficient to protect the plant from O_3 damage. However, the ecotype Cvi-0 also has elevated SA levels and is nevertheless O_3 sensitive, and depletion of SA in crosses with NahG reduced cell death in both Cvi-0 and *rcd1* (Fig. 3A; Rao et al., 2000b). Thus, elevated SA levels in *dnd1* would be predicted to increase cell death and not reduce it. Therefore, it is likely that the lack of O_3-induced cell death in *dnd1* and *rcd1 dnd1* is explained by the lack of a functional HR due to the deficient function of the cation channel rather than through increased SA. K^+ transport is also involved in stomatal regulation, which is a crucial step in determination of O_3 sensitivity (Kollist et al., 2000). Although there are no indications in the literature that AtCNGC2 could have a role in stomatal regulation, and thus that the

dnd1 mutation could affect stomatal conductance, this remains a possibility and requires further study.

O_3-Induced MAP Kinase Activation

Plant MAP kinase cascades are activated by a large number of stimuli, including pathogen infection and O_3 (Zhang and Klessig, 2001; Ahlfors et al., 2004b). Constitutive MAP kinase activation has been shown to lead to HR-like cell death, suggesting that MAP kinase signaling is a part of the ROS-induced PCD (Ren et al., 2002). Inhibition of Ser/Thr kinases (including MAP kinases) with K252a suppressed cell death and phosphatase inhibitors increased cell death in *rcd1* (Fig. 6; Table III), indicating that kinase activation is needed for the early phases of cell death in *rcd1*. However, when the timing and magnitude of cell death in *rcd1* and Col-0 (Overmyer et al., 2000) are compared with the AtMPK6 and AtMPK3 activation (Fig. 8), it is likely that cell death and kinase activation are not directly linked; Col-0 had a high induction of AtMPK3 and AtMPK6 activity but little cell death when compared to *rcd1*. Furthermore, the O_3-sensitive *jar1* has similar MAP kinase activity compared to Col-0 (Ahlfors et al., 2004b). However, it is possible that ROS production and AtMPK6 activation could be linked. The more open stomata of *rcd1* (Ahlfors et al., 2004a) allow more O_3 to enter the plant leaf and to react with the components of the cell wall and plasma membranes, creating more ROS directly from O_3 degradation. This higher oxidative load could also cause the earlier AtMPK6 peak activation in O_3-exposed *rcd1*. The protein phosphatase inhibitor calyculin A, which increased cell death in *rcd1* (Table III), has previously been shown to increase ethylene evolution and ACC synthase activity in tomato significantly without an inductive treatment (Spanu et al., 1994; Tuomainen et al., 1997). In O_3-exposed plants, ethylene is required for the active ROS production responsible for lesion propagation (Overmyer et al., 2000; Moeder et al., 2002). In tobacco, the induction of ethylene biosynthesis takes place through SIPK, the tobacco homolog of Arabidopsis AtMPK6 (Kim et al., 2003), and in Arabidopsis, AtMPK6 directly activates ethylene synthesis by phosphorylating the ACC synthases AtACS6 and AtACS2 (Liu and Zhang, 2004). Thus, the fast and high induction of ethylene biosynthesis involved in the formation of O_3 lesions in *rcd1* (Overmyer et al., 2000) is most likely affected by the earlier peak activity of AtMPK6, since *AtACS6* was also specifically activated by O_3 in *rcd1* (Overmyer et al., 2000). Whether the AtMPK3/6 activation is a result of the increased cell death, or vice versa, requires further study.

Could Multiple Modes of Cell Death Occur in *rcd1*?

The inhibitor treatments reduced, but did not fully block, cell death in ROS-treated *rcd1*. This could be due to the efficacy of the inhibitor treatments, since the action of a given inhibitor is unlikely to completely block its target pathway(s). Another interpretation is that both PCD and necrotic cell death may take place. It has been suggested that both death by rampant oxidation and PCD may occur, depending on the magnitude of O_3-induced oxidative stress (Pell et al., 1997). Furthermore, Rao and Davis (1999) have presented evidence of both O_3-induced necrotic and HR-like cell death, where the mechanism was dependent on genotype. Both *rcd1,* and to a smaller extent Col-0, displayed TUNEL-positive nuclei (Fig. 1), but since the TUNEL assay does not discriminate between random and programmed DNA fragmentation (Collins et al., 1992; Dangl et al., 1996; Pasqualini et al., 2003), it is possible that mosaics of apoptotic and necrotic cells can occur in the same O_3-exposed tissue. Mixtures of cells bearing signs of different modes of death within the same tissue have been described in the study of cell death in mammals (Levin et al., 1999) and have recently been proposed to take place also in plants (Greenberg and Yao, 2004). It could be that signals emanating from the few cells undergoing necrotic cell death by rampant oxidation by O_3-derived ROS may trigger surrounding cells to die by PCD, resulting in large areas of affected tissue and lesion propagation. This is analogous to the penumbra of secondary cell death seen at the periphery of acute hypoxic or traumatic lesions, which has been described extensively in mammals (Jacobson et al., 1997).

A mixture of necrotic and PCD provides a model for some of the results seen in this study and for the mechanism by which O_3 lesion initiation could take place in the oxidative cell death cycle (Overmyer et al., 2003). The higher initial stomatal conductance and the delay in the O_3-induced stomatal closure in *rcd1* (Ahlfors et al., 2004a) allow more O_3 to enter the leaf during the initial phase of the exposure. This could cause more or larger lesion initiations by the direct action of the O_3-derived ROS. However, the presence of characteristic biochemical and morphological markers of PCD in O_3-exposed *rcd1* suggest that the lesion propagation takes placed by hormone-controlled PCD, where the increased activation of MAP kinases is involved in the regulation of hormone biosynthesis. Thus, only lesion propagation would be dependent on active metabolism, ion fluxes, and SA signaling (as indicated by the inhibitor and double-mutant experiments), while the primary cell death observed would be necrotic, caused by the ROS from O_3 degradation. This hypothesis requires further study, especially the role of stomatal function during the early phases of O_3 challenge.

MATERIALS AND METHODS

Plants and Growth Conditions

Arabidopsis (*Arabidopsis thaliana*) was grown on a 1:1 mixture of peat (Type B2; Kekkilä, Tuusula, Finland) and vermiculite at 22°C/18°C (day/night) with 70%/90% relative humidity under short-day (12 h, 250 μmol m^{-2} s^{-1}) irradiance with 5 plants/8 × 8-cm pot. The isolation and genetics of the

rcd1-1 allele used throughout this study has been described previously (Overmyer et al., 2000; Ahlfors et al., 2004a). Twenty-one- to 27-d-old plants (prior to bolting) were used for all experiments. Plants for O_3 exposure and clean-air controls were grown side by side under identical conditions and were selected at random for separation into the two experimental groups. Mutant seeds were obtained from the Arabidopsis Biological Resource Center (ABRC; http://www.arabidopsis.org/abrc/) and the Nottingham Arabidopsis Stock Centre (NASC; http://nasc.nott.ac.uk). Seeds of the transgenic NahG (line B15) in the Col-0 background were a kind gift from Syngenta (Research Triangle Park, NC). *rcd1* NahG, *rcd1 npr1*, *rcd1 jar1*, and *rcd1 dnd1* double-mutant lines were created by crossing the respective plants with a glabrous *rcd1* line as the pollen acceptor. F_1 generation plants were confirmed as true crosses by the presence of trichomes and allowed to self-pollinate. Appropriate homozygous lines were identified from the F_2 populations by PCR screening with dCAPS markers for *rcd1-1*, *jar1-1*, *dnd1*, and *npr1-1*, and by kanamycin resistance screening on plates for the presence of the NahG transgene. All genotypes were confirmed in the F_3 generation.

Superoxide and O_3 Treatments

Extracellular superoxide (XXO in sodium phosphate buffer, 10 mM, pH 7.0) was applied by vacuum infiltration into the apoplast of detached leaves as described (Jabs et al., 1996; Overmyer et al., 2000). Three completely expanded middle-aged leaves from each plant were used. Treatments lasted 18 to 20 h at 22°C in closed 50-mL tubes. The following reagents were included: xanthine (100 μM), xanthine oxidase (0.05 units mL^{-1}), plus inhibitors or other reagents at the concentrations given in Table I. Standard O_3 exposure, 250 nL L^{-1} or 300 nL L^{-1} O_3 for 6 h, unless otherwise noted, with parallel clean-air controls at all time points was as described (Overmyer et al., 2000). At the times indicated, cell death was measured by ion leakage of 2 detached leaves into 5 mL, or whole rosettes into 1 mL, milli-Q water for 1 h, followed by quantification with a conductivity meter (Mettler Toledo, Greifensee, Switzerland). Data are expressed as a percentage of total ions (determined after killing plants by boiling) and are the means of 5 to 10 replicates.

Histological Procedures

For detection of autofluorescent phenolic deposits, plants were cleared by boiling 3 min in alcoholic lactophenol (2:1, 95% ethanol:lactophenol), rinsed in 50% ethanol, and then rinsed twice in water. Cleared leaves were mounted and viewed as by Dietrich et al. (1994). Control samples were microscopically free of autofluorescence in all experiments. For the TUNEL assay, samples were vacuum infiltrated and fixed overnight in 4% paraformaldehyde in phosphate-buffered saline and cryoprotected for 24 h each at 4°C in 15% and then 30% Suc in phosphate-buffered saline. Leaf samples were then submerged in Tissue-Tek OTC Compound 4583 (Miles, Elkhart, IN) and snap frozen in liquid nitrogen prior to cryosectioning (Leitz Kryostat 1720; Ernst Leitz Wetzlar, Wetzlar, Germany). Sections were mounted on Superfrost Plus slides (Menzel-Gläser, Erie Scientific Company, Portsmouth, NH) and stained with the In Situ Cell Death Detection kit (Roche Applied Science, Espoo, Finland), according to the manufacturer's instructions, and counterstained with DAPI. Sections were examined by epifluorescent microscopy (Olympus Provis AX70; Olympus Optical, Tokyo) with standard DAPI and fluorescent filter sets.

Electron Microscopy

O_3-exposed and control leaf samples for electron microscopy were fixed in 2.5% glutaraldehyde in 0.1 M sodium phosphate buffer, pH 7.0, by vacuum infiltration and then overnight at 4°C. Samples were washed and stored at 4°C until further analysis. Samples were then postfixed in 1% osmium tetroxide (EMS, Washington Park, PA), dehydrated through an ethanol series, and embedded in Epon XL 112 (Ladd Research Industries, Williston, VT) and polymerized. Blocks were sectioned on a Reichert ultracut microtome using a diamond knife (Diatome, Bienne, Switzerland) and mounted on copper grid slots. Sections were examined with a transmission electron microscope (JEOL JEM-1200EX; JEOL, Tokyo) at an accelerating voltage of 60 kV.

Hormone Measurements

JA and SA were extracted and quantified with [1,2-^{13}C]JA and [^{13}C1]SA as internal standards as described by Baldwin et al. (1997), with the modifications described by Vahala et al. (2003).

Gene Expression Profiling

Expression of 127 defense-related genes was studied by a cDNA macroarray analysis using cDNA clones and expressed sequence tag clones from the ABRC (Columbus, Ohio). All clones were resequenced. Seventy-five nanograms of each PCR-amplified sample were blotted onto Hybond N+ membranes with a 96-well dot-blot device; 75 ng of oligo$(dT)_{21}$ and pSPORT and pBS plasmids provided the negative controls. The 2 constitutively expressed genes, *ACT2* (At3g18780) and *ACT8* (At1g49240), were each applied to the membrane 4 times. Hybridization and detection were according to Overmyer et al. (2000), except that ^{33}P-dCTP was used for probe labeling. RNA for the analysis was extracted from plants 8 h after the beginning of a 6-h, 250-nL L^{-1} O_3 exposure. The results were normalized by reference to the mean hybridization signals for *ACT2* and *ACT8*. Genes with expression levels below a numerical value of 0.001 in any of the samples were excluded from this analysis. Hybridizations were performed at least twice, and the results represent the mean of the duplicate signals.

Inhibitor Treatments

Inhibitors were used at the concentrations stated in Table I. In XXO experiments, inhibitors were coinfiltrated with the radical-generating system. In O_3 experiments, plants were pretreated 1 h prior to exposure by spraying intact plants with inhibitor solutions. All inhibitor solutions for spraying were dissolved in water with 0.05% Tween 20 to mediate surface wetting. The solvent for stock solutions for K252a, herbimycin A, pepstatin, z-VAD-fmk, and A23187 was DMSO; for E-64 and PMSF, it was ethanol; and the remaining inhibitors were in aqueous solutions. Where appropriate, controls were conducted by adding solvent and Tween 20 to the spray solution or adding solvent to incubation media at the concentrations resulting from dilution of stocks into working solutions. All reagents were from Sigma Aldrich Chemicals (St. Louis), except K252a, E-64, and z-VAD-fmk, which were from Calbiochem (San Diego).

One-way ANOVA tests were performed with two-sided Dunnet's or Tukey's honestly significant difference post-hoc tests as indicated using SPSS 8.0.

MAP Kinase Activity Measurements

Protein extractions, TEY westerns, and immunoprecipitation kinase assays were performed as described previously (Kroj et al., 2003; Ahlfors et al., 2004b).

ACKNOWLEDGMENTS

We are grateful to Prof. Ian Baldwin and Dr. Günter Brader for supplying JA and SA standards, respectively, and to Mika Korva for plant care. We gratefully acknowledge the Department of Ecology and Environmental Sciences at the University of Kuopio, where this work was initiated. We would like to thank the Electron Microscopy Unit of the Institute of Biotechnology at the University of Helsinki for providing laboratory facilities.

Received October 27, 2004; returned for revision December 20, 2004; accepted December 27, 2004.

LITERATURE CITED

Ahlfors R, Lång S, Overmyer K, Jaspers P, Brosché M, Tauriainen A, Kollist H, Tuominen H, Belles-Boix E, Piippo M, et al (2004a) Arabidopsis RADICAL-INDUCED CELL DEATH1 belongs to the WWE protein-protein interaction domain protein family and modulates abscisic acid, ethylene, and methyl jasmonate responses. Plant Cell **16:** 1925–1937

Ahlfors R, Macioszek V, Rudd J, Brosché M, Schlichting R, Scheel D, Kangasjärvi J (2004b) Stress hormone-independent activation and nuclear translocation of mitogen-activated protein kinases in *Arabidopsis thaliana* during ozone exposure. Plant J **40:** 512–522

Asai T, Tena G, Plotnikova J, Willmann MR, Chiu WL, Gomez-Gomez L,

Boller T, Ausubel FM, Sheen J (2002) MAP kinase signalling cascade in Arabidopsis innate immunity. Nature **415:** 977–983

Baldwin IT, Zhang Z-P, Diab N, Ohnmeiss TE, McCloud ES, Lynds GY, Schmelz EA (1997) Quantification, correlations and manipulations of wound-induced changes in jasmonic acid and nicotine in *Nicotiana sylvestris*. Planta **201:** 397–404

Bowler C, Fluhr R (2000) The role of calcium and activated oxygen as signals for controlling cross-tolerance. Trends Plant Sci **5:** 241–246

Castillo FJ, Heath RL (1990) Ca^{2+} transport in membrane vesicles from pinto bean leaves and its alteration after ozone exposure. Plant Physiol **94:** 788–795

Cessna SG, Low PS (2001) An apoplastic Ca^{2+} sensor regulates internal Ca^{2+} release in Aequorin-transformed tobacco cells. J Biol Chem **276:** 10655–10662

Chang L, Karin M (2001) Mammalian MAP kinase signalling cascades. Nature **410:** 37–40

Clayton H, Knight MR, Knight H, McAinsh MR, Hetherington AM (1999) Dissection of the ozone-induced calcium signature. Plant J **17:** 575–579

Clough SJ, Fengler KA, Yu IC, Lippok B, Smith RK Jr, Bent AF (2000) The *Arabidopsis dnd1* ''defense, no death'' gene encodes a mutated cyclic nucleotide-gated ion channel. Proc Natl Acad Sci USA **97:** 9323–9328

Collins RJ, Harmon BV, Gobe GC, Kerr JFR (1992) Internucleosomal DNA clevage should not be the sole criterion for identifying apoptosis. Int J Radiat Biol **61:** 451–453

Dangl JL, Dietrich RA, Richberg MH (1996) Death don't have no mercy: cell death programs in plant-microbe interactions. Plant Cell **8:** 1793–1807

Dat JF, Pellinen R, Beeckman T, Van De Cotte B, Langebartels C, Kangasjärvi J, Inze D, Van Breusegem F (2003) Changes in hydrogen peroxide homeostasis trigger an active cell death process in tobacco. Plant J **33:** 621–632

Devadas SK, Enyedi A, Raina R (2002) The *Arabidopsis hrl1* mutation reveals novel overlapping roles for salicylic acid, jasmonic acid and ethylene signalling in cell death and defence against pathogens. Plant J **30:** 467–480

Dietrich RA, Delaney TP, Uknes SJ, Ward ER, Ryals JA, Dangl JL (1994) Arabidopsis mutants simulating disease resistance response. Cell **77:** 565–577

Durner J, Shah J, Klessig DF (1997) Salicylic acid and disease resistance in plants. Trends Plant Sci **2:** 266–274

Fujibe T, Saji H, Arakawa K, Yabe N, Takeuchi Y, Yamamoto KT (2004) A methyl viologen-resistant mutant of Arabidopsis, which is allelic to ozone-sensitive *rcd1*, is tolerant to supplemental ultraviolet-B irradiation. Plant Physiol **134:** 275–285

Garcia-Calvo M, Peterson EP, Leiting B, Rue R, Nicholson DW, Thornberry NA (1998) Inhibition of human caspases by peptide-based and macromolecular inhibitors. J Biol Chem **273:** 32608–32613

Greenberg JT, Yao N (2004) The role and regulation of programmed cell death in plant-pathogen interactions. Cell Microbiol **6:** 201–211

Hatsugai N, Kuroyanagi M, Yamada K, Meshi T, Tsuda S, Kondo M, Nishimura M, Hara-Nishimura I (2004) A plant vacuolar protease, VPE, mediates virus-induced hypersensitive cell death. Science **305:** 855–858

He SYH, Huang H-C, Collmer A (1993) *Pseudomonas syringae* pv syringe harpin Pss: a protein that is secreted via the Hrp pathway and elicits the hypersensitive response in plants. Cell **73:** 1255–1266

Heath RL, Taylor GE Jr (1997) Physiological processes and plant responses to ozone exposure. *In* H Sandermann Jr, AR Wellburn, RL Heath, eds, Forest Decline and Ozone, Ecological Studies, Vol 127. Springer, Heidelberg, pp **317–368**

Jabs T, Dietrich RA, Dangl JL (1996) Initiation of runaway cell death in an *Arabidopsis* mutant by extracellular superoxide. Science **273:** 1853–1856

Jacobson MD, Weil M, Raff MC (1997) Programmed cell death in animal development. Cell **88:** 347–354

Kangasjärvi J, Talvinen J, Utriainen M, Karjalainen R (1994) Plant defense systems induced by ozone. Plant Cell Environ **17:** 783–794

Kim CY, Liu Y, Thorne ET, Yang H, Fukushige H, Gassmann W, Hildebrand D, Sharp RE, Zhang S (2003) Activation of a stress-responsive mitogen-activated protein kinase cascade induces the biosynthesis of ethylene in plants. Plant Cell **15:** 2707–2718

Koch JR, Creelman RA, Eshita SM, Seskar M, Mullet JE, Davis KR (2000) Ozone sensitivity in hybrid poplar correlates with insensitivity to both salicylic acid and jasmonic acid. The role of programmed cell death in lesion formation. Plant Physiol **123:** 487–496

Kollist H, Moldau H, Mortensen L, Rasmussen SK, Jorgensen LB (2000) Ozone flux to plasmalemma in barley and wheat is controlled rather by stomata than by direct reaction of ozone with apoplastic ascorbate. J Plant Physiol **156:** 645–651

Kroj T, Rudd JJ, Nurnberger T, Gabler Y, Lee J, Scheel D (2003) Mitogen-activated protein kinases play an essential role in oxidative burst-independent expression of pathogenesis-related genes in parsley. J Biol Chem **278:** 2256–2264

Lam E (2004) Controlled cell death, plant survival and development. Nat Rev Mol Cell Biol **5:** 305–315

Langebartels C, Kangasjärvi J (2004) Ethylene and jasmonate as regulators of cell death in disease resistance. *In* H Sandermann Jr, ed, Molecular Ecotoxicology of Plants, Ecological Studies, Vol 170. Springer, Heidelberg, pp 75–110

Leng Q, Mercier RW, Hua B-G, Fromm H, Berkowitz GA (2002) Electrophysiological analysis of cloned cyclic nucleotide-gated ion channels. Plant Physiol **128:** 400–410

Leng Q, Mercier RW, Yao W, Berkowitz GA (1999) Cloning and first functional characterization of a plant cyclic nucleotide-gated cation channel. Plant Physiol **121:** 753–761

Levin S, Bucci TJ, Cohen SM, Fix AS, Hardisty JF, LeGrand EK, Maronpot RP, Trump BF (1999) The nomenclature of cell death: recommendations of an ad hoc committee of the society of toxicologic pathologists. Toxicol Pathol **27:** 484–490

Levine A, Pennell RI, Alvarez ME, Palmer R, Lamb C (1996) Calcium-mediated apoptosis in a plant hypersensitive disease resistance response. Curr Biol **6:** 427–437

Liu Y, Zhang S (2004) Phosphorylation of 1-aminocyclopropane-1-carboxylic acid synthase by MPK6, a stress-responsive mitogen-activated protein kinase, induces ethylene biosynthesis in Arabidopsis. Plant Cell **16:** 3386–3399

Lorrain S, Vailleau F, Balague C, Roby D (2003) Lesion mimic mutants: keys for deciphering cell death and defense pathways in plants? Trends Plant Sci **8:** 263–271

Mittler R, Simon L, Lam E (1997) Pathogen-induced programmed cell death in tobacco. J Cell Sci **110:** 1333–1344

Moeder W, Barry CS, Tauriainen A, Betz C, Tuomainen J, Utriainen M, Grierson D, Sandermann H Jr, Langebartels C, Kangasjärvi J (2002) Ethylene synthesis regulated by bi-phasic induction of ACC synthase and ACC oxidase genes is required for H_2O_2 accumulation and cell death in ozone-exposed tomato. Plant Physiol **130:** 1918–1926

Örvar BL, McPherson J, Ellis BE (1997) Pre-activating wounding response in tobacco prior to high-level ozone exposure prevents necrotic injury. Plant J **11:** 203–212

Overmyer K, Brosché M, Kangasjärvi J (2003) Reactive oxygen species and hormonal control of cell death. Trends Plant Sci **8:** 335–342

Overmyer K, Tuominen H, Kettunen R, Betz C, Langebartels C, Sandermann H Jr, Kangasjärvi J (2000) The ozone-sensitive *Arabidopsis rcd1* mutant reveals opposite roles for ethylene and jasmonate signaling pathways in regulating superoxide-dependent cell death. Plant Cell **12:** 1849–1862

Pasqualini S, Piccioni C, Reale L, Ederli L, Della Torre G, Ferranti F (2003) Ozone-induced cell death in tobacco cultivar Bel W3 plants. The role of programmed cell death in lesion formation. Plant Physiol **133:** 1122–1134

Pell EJ, Schlagnhaufer CD, Arteca RN (1997) Ozone-induced oxidative stress: mechanisms of action and reaction. Physiol Plant **100:** 264–273

Rao MV, Davis KR (1999) Ozone-induced cell death occurs via two distinct mechanisms in *Arabidopsis*: the role of salicylic acid. Plant J **17:** 603–614

Rao MV, Davis KR (2001) The physiology of ozone-induced cell death. Planta **213:** 682–690

Rao MV, Koch JR, Davis KR (2000a) Ozone: a tool for probing programmed cell death in plants. Plant Mol Biol **44:** 345–358

Rao MV, Lee HI, Creelman RA, Mullet JA, Davis KR (2000b) Jasmonic acid signalling modulates ozone-induced hypersensitive cell death. Plant Cell **12:** 1633–1646

Ren D, Yang H, Zhang S (2002) Cell death mediated by MAPK is associated with hydrogen peroxide production in *Arabidopsis*. J Biol Chem **277:** 559–565

Rojo E, Martiìn R, Carter C, Zouhar J, Pan S, Plotnikova J, Jin H, Paneque M, Saìnchez-Serrano JJ, Baker B, et al (2004) VPEγ exhibits a caspase-

like activity that contributes to defense against pathogens. Curr Biol **14:** 1897–1906

Sandermann H Jr, Ernst D, Heller W, Langebartels C (1998) Ozone: an abiotic elicitor of plant defence reactions. Trends Plant Sci **3:** 47–50

Spanu P, Grosskopf DG, Felix G, Boller T (1994) The apparent turnover of 1-aminocyclopropane-1-carboxylate synthase in tomato cells is regulated by protein phosphorylation and dephosphorylation. Plant Physiol **106:** 529–535

Tuomainen J, Betz C, Kangasjärvi J, Ernst D, Yin ZH, Langebartels C, Sandermann H Jr (1997) Ozone induction of ethylene emission in tomato plants: regulation by differential transcript accumulation for the biosynthetic enzymes. Plant J **12:** 1151–1162

Tuominen H, Overmyer K, Keinänen M, Kollist H, Kangasjärvi J (2004) Mutual antagonism of ethylene and jasmonic acid regulates ozone-induced spreading cell death in Arabidopsis. Plant J **39:** 59–69

Vahala J, Ruonala R, Keinänen M, Tuominen H, Kangasjärvi J (2003) Ethylene insensitivity modulates ozone-induced cell death in birch. Plant Physiol **132:** 185–195

Vercammen D, Van De Cotte B, De Jaeger G, Eeckhout D, Casteels P, Vandepoele K, Vandenberghe I, Van Beeumen J, Inze D, Van Breusegem F (2004) Type-II metacaspases Atmc4 and Atmc9 of *Arabidopsis thaliana* cleave substrates after arginine and lysine. J Biol Chem **279:** 45329–45336

Vranová E, Inzé D, Van Breusegem F (2002) Signal transduction during oxidative stress. J Exp Bot **53:** 1227–1236

Watanabe N, Lam E (2004) Recent advance in the study of caspase-like proteases and Bax inhibitor-1 in plants: their possible roles as regulator of programmed cell death. Mol Plant Pathol **5:** 65–70

Wohlgemuth H, Mittelstrass K, Kschieschan S, Bender J, Weigel H-J, Overmyer K, Kangasjärvi J, Langebartels C, Sandermann H Jr (2002) Activation of an oxidative burst is a general feature of sensitive plants exposed to the air pollutant ozone. Plant Cell Environ **25:** 717–726

Zhang S, Klessig DF (2001) MAPK cascades in plant defense signaling. Trends Plant Sci **6:** 520–527